Journal of Inflammation Research

Dovepress
Taylor & Francis Group

Open Access Full Text Article

ORIGINAL RESEARCH

Integrating Extracellular Vesicles Proteomics and Clinical Parameters to Develop a High-Precision Predictive Model for Severe Asthma

Yuhao Qian[1,*], Fang Wang[2,*], Jiameng Gao[2], Zhilong Jiang[2], Xiwen Gao[1], Zhihong Chen[3]

[1]Department of Respiratory and Critical Care Medicine, Minhang Hospital, Fudan University, Shanghai, People's Republic of China; [2]Department of Respiratory and Critical Care Medicine of Zhongshan Hospital, Shanghai Institute of Respiratory Disease, Fudan University, Shanghai, People's Republic of China; [3]Department of Pulmonary and Critical Care Medicine, Xinhua Hospital, Shanghai Jiaotong University School of Medicine, Shanghai, People's Republic of China

*These authors contributed equally to this work

Correspondence: Zhihong Chen, Department of Pulmonary and Critical Care Medicine, Xinhua Hospital, Shanghai Jiaotong University School of Medicine, Shanghai, People's Republic of China, Email chenzhihong@xinhuamed.com.cn; Xiwen Gao, Department of Respiratory and Critical Care Medicine, Minhang Hospital, Fudan University, Shanghai, People's Republic of China, Email xiwengao@sina.com

Introduction: This study aimed to identify biomarkers and develop a predictive model for distinguishing severe asthma (SA) from non-severe asthma (NSA) by integrating clinical data and extracellular vesicles (EVs) proteomics.

Methods: Plasma-derived EVs were isolated from 44 individuals, including 15 healthy controls, 15 SA patients, and 14 NSA patients. Proteomic profiling of EVs was performed using proximity barcoding assay (PBA). Clinical indicators such as FEV1/FVC ratio, DLCO% predicted, and blood neutrophil count were recorded. A multivariate model incorporating both clinical and EV-derived protein data was constructed and evaluated using ROC curve analysis. Candidate biomarkers were further validated in cell-based and murine SA models.

Results: Although total EV counts and protein load did not differ significantly across groups, specific EV proteins (eg, SELL, PECAM1, ITGB3, CD9) were consistently elevated. Notably, protein combinations such as ITGB3&CLDN1 and ESAM&ITGA6 showed strong discriminatory power between SA and NSA (AUC > 0.8). The integrative model combining clinical metrics and EV proteins (IL6, NGFR, NFASC, PCDHA1) achieved a high predictive accuracy (AUC = 0.97 ± 0.075). Expression of IL6, NGFR, and NFASC was significantly upregulated in SA cellular and animal models, aligning with patient data.

Conclusion: This study presents a reliable multi-parameter model for distinguishing severe from non-severe asthma, leveraging both clinical indicators and EV proteomics. These findings support the potential of EV-based biomarkers in early diagnosis and personalized management of SA.

Keywords: extracellular vesicle, EVs, proximity barcoding assay, PBA, asthma, severe asthma, *Aspergillus flavus*

Introduction

Asthma, a heterogeneous chronic airway disease affecting over 300 million people globally, poses substantial clinical challenges due to its unpredictable exacerbations and suboptimal control rates.[1–3] In China, approximately 30 million people suffer from asthma, with over 50% experiencing uncontrolled symptoms and disproportionately high mortality rate.[4] While asthma diagnosis and monitoring predominantly depend on symptoms and lung function tests according to the Global Initiative for Asthma (GINA) guidelines,[5,6] these approaches have limitations due to confounding variables, notably their inability to objectively stratify disease severity. Furthermore, intervention strategies for severe asthma have been insufficiently studied.[7] In recent years, biomarkers have become increasingly important in the diagnosis and management of respiratory diseases,[8,9] and precision asthma management requires developing companion diagnostics that match specific inflammatory endotypes to guide targeted biologics.[10,11] To achieve this goal, identifying validated biomarkers is essential for early detection and improved outcomes through mechanism-based interventions.

Received: 4 August 2025
Accepted: 11 December 2025
Published: 23 December 2025

Graphical Abstract

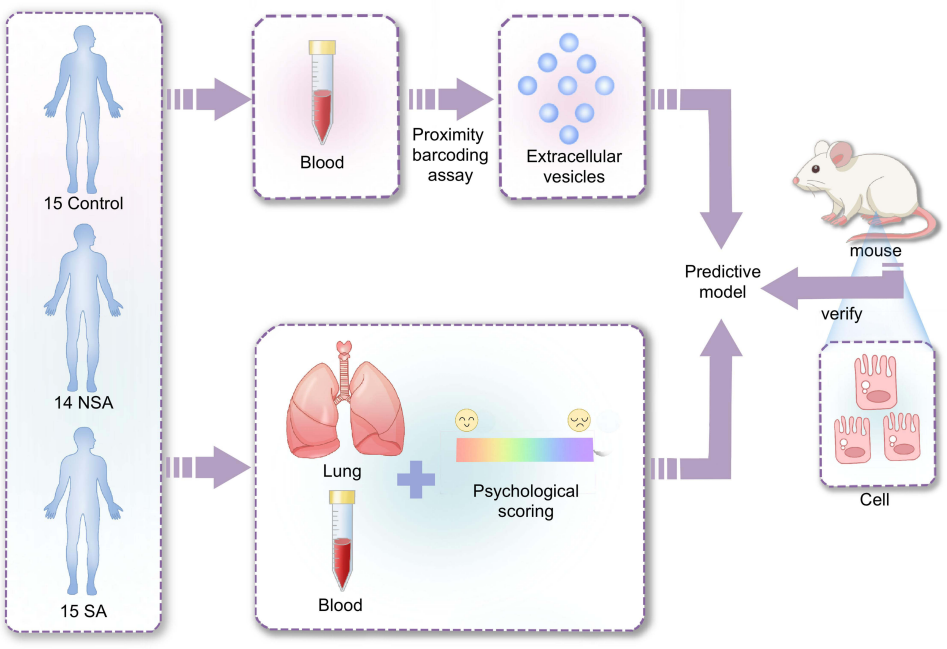

Extracellular vehicles (EVs), especially exosomes, have become promising biomarker repositories due to their stability in circulation and molecular cargo reflecting cellular pathophysiology.[12] EVs are detectable in diverse biological fluids — including plasma, urine, semen, bronchial fluid, synovial fluid, and tears — and transport a heterogeneous cargo comprising proteins, metabolic enzymes, and nucleic acids such as DNA, mRNA, microRNAs (miRNAs), long noncoding RNAs (lncRNAs), and circular RNAs (circRNAs).[13,14] In asthma, EVs are actively released by diverse immune cells, including eosinophils, mast cells, dendritic cells, T lymphocytes, neutrophils, and macrophages, as well as structural cells such as airway epithelial cells, driving inflammatory pathogenesis. For instance, M2 macrophage-derived exosomes regulate the imbalance in epithelial proliferation and apoptosis in asthma, reducing inflammation and mitigating tissue remodeling.[15] Moreover, eosinophil-derived EVs in asthma patients enhance nitric oxide and reactive oxygen species production, promote chemotaxis, and upregulate adhesion molecules on eosinophils.[16,17] In addition, recent comparative proteomics of immune cell-derived small EVs (sEVs) has identified TH2-associated biomarkers capable of differentiating T2-high and T2-low asthma endotypes.[18–20] However, the existing studies mainly focus on single-omics methods, ignoring the synergistic effects of integrating exosome biomarkers with multi-dimensional clinical indicators.[21] The existing predictive models also rely solely on clinical data to predict severe asthma in children.[22]

To address this, we hypothesize that a machine learning-driven model combining exosome proteomics and clinical parameters can achieve superior accuracy in predicting SA. Using a PBA, we systematically compared EV profiles across SA, NSA, and healthy controls. Building on these findings, our study established a multidimensional predictive model combining clinical and exosome biomarkers for asthma severity stratification. To functionally validate the identified biomarkers, we developed an *Aspergillus fumigatus*-induced experimental SA model, enabling cross-validation of exosome-derived markers.

Materials and Methods

Selection of Clinical Samples Collection

The inclusion criteria were based on the diagnostic standards of the Global Initiative for Asthma (GINA).[5] Patients in the severe asthma group (SA) met one of the following two criteria: (1) use of asthma medications (high-dose ICS combined with LABA or leukotriene modifiers/theophylline) or systemic corticosteroids for more than 50% of the time to maintain symptom control; or (2) failure to achieve control despite the use of these medications. Patients in the non-severe asthma group (NSA) met the general inclusion criteria for asthma but did not fulfill both criteria required for classification as severe asthma.

The exclusion criteria were as follows: no severe systemic diseases or serious infections in other parts of the body within the past four weeks; no use of antibiotics, phenytoin sodium, cyclosporine, lipid-lowering drugs, oral contraceptives, atropine, or other related medications within the past four weeks; and not being pregnant or breastfeeding.

This study was conducted in the Department of Respiratory Medicine at Zhongshan Hospital of Fudan University. Plasma samples were collected from 15 healthy subjects and 29 asthma patients, including 15 patients with severe asthma (SA) and 14 with non-severe asthma (NSA). All procedures were approved by the Ethical Committee of Fudan University Zhongshan Hospital for clinical discovery and validation studies (B2018-196R). All participants provided informed consent prior to their inclusion in the study. The study was conducted in accordance with the principles of the Declaration of Helsinki.

Basic information about these sample contributors is located in Table 1.

Peripheral Blood Sample Collection and Pretreatment

Peripheral blood was drawn from patients at the onset of illness and at the time of stabilization to ensure that a competent sample was obtained. Eight milliliters of blood were drawn from the median elbow vein of the left arm of patients and healthy individuals, placed in EDTA anticoagulation tubes, and stored at 4 °C (for no more than 4 hours). Samples were centrifuged at 300 × g for 15 minutes, and the supernatant was collected. The supernatant was then centrifuged again at 300 × g at 4 °C for 15 minutes. The resulting supernatant was collected and stored at −80 °C for later use.

Proximity Barcoding Assay (PBA) Process for Detection of Single EV Epitope Proteins

The EV-containing sample is first mixed with the antibody panel, which specifically recognizes the protein. A 96-well plate with an EV affinity capture coating on the surface of the plate is used, and the sample and antibody panel are added to the plate. The EV is captured, the EV tag template solution is added, and the DNA fragment label on the antibody hybridizes to a specific position on the EV tag template. The DNA fragments are then constructed into DNA libraries and sequenced. Sequencing sequence tags are extracted to form the original input file for further analysis. The PBA tests were designed according to protocols from Vesicode AB (Solna, Sweden) and were performed at Secretech (Shenzhen, China).

Protein Expression Normalization

Raw counts of protein expression profiles were normalized using the M-value trimmed mean (TMM) in the "edgeR" R package (PMID: 19910308). The normalized protein profiles were subjected to principal component analysis (PCA) downscaling using the "FactoMineR" R package and visualized using the "factoextra" R package. Specifically, the PCA analysis used protein features that were differentially expressed between the three groups. Statistical significance was determined using the Kruskal–Wallis test ($p < 0.05$).

Identification of Differentially Expressed Proteins

To identify proteins that differed between any two groups (control vs SA group; control vs NSA group; SA group vs NSA group), we used the Wilcoxon test to calculate statistical significance. Proteins with $P < 0.05$ and absolute value of log change > 0.3 were considered significant. We used volcano plots based on the "ggplot2" R package to show significant proteins.

Table 1 Personal Information and Clinical Data of Severe Asthmatics (SA) and Non-Severe Asthmatics (NSA)

	NSA (N=14)	SA (N=15)	P-value
Demography and underlying characteristics			
Sex(male)(N,%)	5 (35.7%)	7 (46.7%)	0.825
Age(years)(mean±SD)	48.7±13.9	55.7±10.6	0.141
BMI(kg/m^2)(mean±SD)	22.9±4.00	22.8±2.84	0.956
Age at first diagnosis(years)(mean±SD)	41.7±12.1	28.1 ±19.0	0.029*
Smoking(Yes)(n,%)	2 (14.3%)	1 (6.7%)	0.95
Occupational dust exposure(Yes)(n,%)	1 (7.1%)	1 (6.7%)	1
Long-term use of drugs for other diseases(Yes)(n,%)	0 (0%)	6 (40.0%)	0.028*
Disease Characteristics and Treatment			
Annual exacerbation in last years(times)(median[min,max])	0[0–0.75]	1[0,2]	0.009*
High-dose ICS inhalation(Yes)(n,%)	0 (0%)	15 (100%)	<0.001*
Oral OCS(Yes)(n,%)	0 (0%)	7 (46.7%)	0.012*
Allergens detection(n,%)			
Negative	7 (50.0%)	10 (66.7%)	0.28
Positive	7 (50%)	4 (26,6%)	
Undected	0 (0%)	1 (6.7%)	
Trigger exposure, n (%)	5 (35.7%)	13 (86.7%)	0.015*
Lung Function and Biomarkers			
FVC(L)(mean±SD)	3.29±0.897	2.72±0.935	0.107
FVC%pre(%)(mean±SD)	95.7±13.8	80.6±21.0	0.031*
FEV1(L)(mean±SD)	2.51±0.710	1.46±0.775	<0.001*
FEV%pre(%)(mean±SD)	90.5±17.3	54.6±25.0	<0.001*
FEV1/FVC(%)(mean±SD)	76.3±8.83	51.8±13.7	<0.001*
FEV1/FVC%pre(%)(mean±SD)	93.6±10.1	64.5±16.5	<0.001*
DLCO(mL/min/kPa)(mean±SD)	7.88±1.81	5.92±2.01	0.014*
DLCO%pre(%)(mean±SD)	110±12.5	85.9±25.5	0.005*
FEV1CHG(L)(mean±SD)	0.156±0.239	0.138±0.156	0.81
FEV1%CHG(%)(mean±SD)	8.13±16.7	12.4±10.3	0.425
FeNO(ppb)(median[min,max])	40.0 [23.0, 92.0]	47.0 [18.0, 121]	0.489
Blood neutrophil count(10^9/L)(median[min,max])	2.95 [1.90, 4.70]	5.20 [2.10, 9.60]	0.002*
Blood eosinophil count(10^9/L)(median[min,max])	0.200 [0.0700, 0.810]	0.200 [0, 0.930]	0.537
Percentage of blood neutrophils(%)(mean±SD)	54.7±6.83	61.3±7.52	0.021*
Percentage of blood eosinophils(%)(median[min,max])	4.05 [1.80, 12.0]	2.10 [0, 10.8]	0.138
IgE(IU/mL)(median[min,max])	27.0 [9.00, 693]	77.0 [14.0, 1910]	0.387
Psychological assessment and quality of life			
ACT(score)(mean±SD)	20.0±3.09	19.1±4.35	0.509
ACQ(score)(mean±SD)	5.86±3.74	11.3±6.31	0.009*
Mini-AQLQ(score)(mean±SD)	45.8±14.1	44.9±12.7	0.866
Depression (DASS-21)(median[min,max])	3.50 [0, 10.0]	5.00 [0, 10.0]	0.486
Anxiety (DASS-21)(median[min,max])	3.00 [0, 9.00]	4.00 [0, 10.0]	0.937
Stress (DASS-21)(median[min,max])	6.00 [0, 19.0]	9.00 [0, 18.0]	0.675

Notes: Normally distributed continuous data are presented as mean ± SD; non-normally distributed as median [min, max]; categorical data as n (%). *P < 0.05. Chi-square test or Fisher's exact test for categorical data;*t*-test or Mann–Whitney *U*-test for continuous data. Depression, Anxiety and Stress was tested using the DASS-21 questionnaire scores. The ACT and ACQ are the Asthma Control Test and Asthma Control Questionnaire.

Protein-Protein Interaction Analysis

To identify potential interactions between differentially expressed proteins, we performed protein-protein interaction analyses between paired groups using the "STRINGdb" R package (default parameters are https://rpubs.com/HWH/913747). Specifically, version 11.5 of the STRING database was used.

Gene Set Enrichment Analysis

To identify signaling pathway dysregulation that may be caused by differentially expressed proteins, we performed an enrichment analysis of the list of up-regulated proteins in each group on the Metascape website (https://metascape.org/gp/index.html#/main/step1) (PMID. 30944313).

Time Series Analysis

To further identify proteins whose expression patterns varied with asthma severity, we performed a time series analysis using the "Mfuzz" R package (PMID: 18084642). Briefly, we used normalized protein expression profiles to calculate the average expression of each protein in each group, which was further used for fuzzy c-means clustering analysis. Specifically, the number of clusters was set to 6 in this example.

Prediction Model

To build predictive models that would distinguish SA or NSA from controls, we utilized significant difference features ($P < 0.05$) to build the models. The random forest (RF) model was constructed from 501 estimation trees, each containing 10% of the total features. An iterative feature elimination (IFE) step was used to filter features and optimize the performance of subsequent RF models (PMID: 34031391, PMID: 37944495, PMID: 38243343). The most important features from the best-performing models were selected as "core features" and considered marker proteins. Metrics to assess model performance included area under the curve (AUC), accuracy, sensitivity, specificity, precision, and F1 score. To test whether the performance of the RF model can be improved when clinical factors are added to distinguish SA from NSA, we constructed an RF model that combines labeled proteins and clinical factors using the same hyperparameters as the discovery RF model. (As for the independent validation in the other cohort, the RF models in the validation cohort are constructed with the same hyperparameters as the training RF models).

Clinical Correlation

We compared clinical factors for SA and NSA and determined their statistical significance using chi-square tests or Fick's exact tests (where available). To assess the predictive performance of a clinical factor, we assessed the area under the curve (AUC) of a clinical factor using the "pROC" R package. Spearman correlation analysis was used to assess the correlation between clinical factors and proteins.

Cell Culture and Grouping

Mouse lung epithelial cells (MLE12) were obtained from Shanghai Shujing Biotechnology Co. (Shanghai, China) and cultured in Dulbecco's Modified Eagle Medium/Nutrient Mixture F-12 (DMEM/F12, BIOAGRIO, USA). All culture mediums were complete medium supplemented with 10% fetal bovine serum (BIOAGRIO, LTD, USA), penicillin (100 μg/mL), and strepto-mycin (100 μg/mL) (Beyotime Biotechnology, Jiangsu, China). All of the cells were cultured under standard culture conditions (37 ◦C, 5% CO2). Cells were treated in *Aspergillus fumigatus* (Af) (10ug/mL)(Greer Lab, USA) and Lipopolysaccharide (LPS) (10ug/mL)(Sigma, USA) co-intervention for 48h.

Aspergillus fumigatus-Induced Severe Mouse Model

All animal experiments were performed in accordance with the Guide for the Care and Use of Laboratory Animals published by the US National Institutes of Health (NIH Publication No. 85–23, revised 2011), and were approved by the Animal Ethics Committee of Zhongshan Hospital, Fudan University. Female C57BL/6J mice (6 weeks old, weight about 20 g) were purchased from Nanjing Charles River Co. Mice were housed in SPF facilities with free access to standard feed and water, The mice were housed in an SPF facility with free access to standard feed and water, a rearing environment (22 ◦C ± 2 ◦C, 55% ± 5% humidity) with a 12 h light/dark cycle. Animals were isolated and acclimatized for one week before use. A total of 10 mice were divided into 2 groups of 5 mice each: Control(Con), *Aspergillus fumigatus* (Af)+Lipopolysaccharide (LPS) group. This study was slightly modified compared to the traditional asthma modeling approach. Mice in the Af+LPS group were injected intraperitoneally with a mixture of 20ul of Af (1mg/mL)

(*Aspergillus fumigatus*, Greer Lab, USA), 80ul of alum adjuvant (77161, Thermo Fisher, USA), and 100ul of physiological saline at the sensitization stage on day 1 and day 7, respectively. During the excitation phase on days 15, 16, and 17, 25ul of Af and 5ul of LPS (1mg/mL) (L2880, Sigma, USA) were intubated by tracheal tube and taken on day 19. For the Con group, all the Af was replaced with an equal amount of saline.

Western Blot Analysis

Proteins were treated with 10% SDS-PAGE gel (Yamei, Shanghai, China) and electroblotted onto a PVDF membrane (Roche, UK). After blocking, the membrane was incubated with GAPDH primary antibody (Proteintech, Wuhan, China, 1:10,000), NGFR primary antibody (T55411, Abmart, China, 1:2000), or NFASC primary antibody (PS03571, Abmart, China, 1:2000) and incubated at 4 ◦C overnight. The membranes were then washed with TBST and incubated with horseradish peroxidase-coupled goat anti-rabbit IgG (SA00001-2, Proteintech, Wuhan, 1:4000) at room temperature for 2 h. Colors were developed using a chemiluminescent reagent (1705061, Bio-Rad, USA), and Image-Pro Plus 6.0 software was used for the GAPDH was used as a reference.

Hematoxylin-Eosin (H&E) and Periodic Acid-Schiff (PAS) Staining

Lung tissues were sectioned (4 μm thick) and stained with hematoxylin and eosin (H&E). Peribronchial inflammatory cell infiltration was as follows: 0, no inflammatory cell infiltration was seen; 0.5, infiltration area was less than 5% of the total area; 1, 5%-10%; 1.5, 10%-15%; 2, 15%-20%; 2.5, 20%-25%; 3, 25%-30%; 3.5, 30%-40%; and 4, >40%. Eosinophilic infiltration of vessels and peribronchioles: 0, not seen; 0.5, <5%; 1,5%-10%; 1.5, 10%-15%; 2, >15%.To identify mucus-containing cells, slides were stained with Schiff periodate (PAS). The following criteria were used to determine the abundance of PAS-positive cells in the airway: 0, <5% of positive cells; 1, 5–25%; 2, 25–50%; 3, 50–75%; 4, >75%.

Enzyme-Linked Immunosorbent Assay (ELISA)

An enzyme-linked immunosorbent assay (ELISA) was used to determine IL-6 in Cell culture fluid (R&D, USA).

Statistical Analysis

All statistical analyses were performed using GraphPad Prism 9 (GraphPad Software, San Diego, CA), R (v4.3.0), and Python (v3.7.6). Data are presented as mean ± standard deviation (SD). For comparisons between two groups, unpaired Student's *t*-test was used; for comparisons among multiple groups, one-way analysis of variance (ANOVA) followed by Tukey's post hoc test was performed. The specific statistical tests applied to each dataset are detailed in the corresponding figure legends and methods sections. A P-value < 0.05 was considered statistically significant.

Statistical significance is indicated as follows:

ns, not significant ($P \geq 0.05$); * $P < 0.05$; ** $P < 0.01$; *** $P < 0.001$; **** $P < 0.0001$.

Result

The Clinical and Demographic Characteristics of Patients with Asthma

A total of 44 participants were initially enrolled in this study, including healthy controls (n=15), SA (n=15) patients, and NSA (n=14) patients. No differences in age, sex, smoking status, BMI, Allergens, ACT score, IgE, or occupational dust exposure were found in the NSA and SA groups. The age of initial asthma diagnosis was significantly younger in the SA group compared to the NSA group ($p = 0.029$). It may indicate that patients with early-onset asthma are more likely to develop severe asthma. Furthermore, patients with SA demonstrated significantly more identifiable onset triggers compared to those with NSA ($p = 0.015$). NSA patients had significantly higher values in FVC% predicted ($p = 0.031$), FEV1 ($p < 0.001$), FEV1% predicted ($p < 0.001$), FEV1/FVC ratio ($p < 0.001$), FEV1/FVC% predicted ($p < 0.001$), DLCO ($p = 0.014$), and DLCO% predicted ($p = 0.005$) compared to SA patients. However, there was no difference in psychological scores between NSA and SA patients in terms of depression, anxiety, and stress. Consistent

with prior evidence,[19] hematological analysis indicated elevated leukocyte counts and percentages in SA patients relative to the NSA group. All statistical outcomes are systematically presented in Table 1.

High-Throughput Profiling of Extracellular Vesicles via Proximity Barcoding Assay

EVs extraction and processing procedures are illustrated in Figure 1A. Using PBA, we quantified EV counts, total protein content, and the average protein carried per EV in the three groups (Figure 1B–D). No significant differences were observed in these parameters between groups. Following data normalization with the trimmed mean of M-values (TMM) method to correct for technical variability, global protein expression profiles were visualized via a dot plot (Figure 1E). Integrins (ITGB3, ITGB1, ITGA6, ITGA2), adhesion molecules (PECAM1, SELL), and tetraspanins (CD9, CD151) exhibited consistently elevated expression across all cohorts compared to other panel proteins, suggesting their potential roles as conserved EV markers in asthma pathophysiology.

Identification of EV Protein Signatures for Severe Asthma Prediction and Subpopulation Profiling

Differentially expressed proteins among the sample groups were identified and visualized through a heatmap, followed by hierarchical clustering to reveal similarities between samples (Figure 2A). As the main goal of this study is to enable early prediction and intervention for severe asthma, particular attention was given to the comparison between the NSA and SA groups. The predictive performance of protein markers was evaluated using ROC curve analysis across different group comparisons: control vs NSA (Figure 2B), NSA vs SA (Figure 2C), and control vs SA (Figure 2D). Among them, PCDHA1 was used as a representative marker in the NSA vs SA comparison, but its area under the ROC curve (AUC) was only 0.733, indicating limited value as a single diagnostic indicator. To improve prediction accuracy, combinations of protein markers were analyzed. Notably, nine protein pairs showed strong predictive ability with AUC values exceeding 0.8, including ITGB3&CLDN1, CLDN3&DSCAML1, ULBP1&ANAX1, FOLH1&ITGB2, SIGLEC5&ITGA6, CD274&PECAM1, NT5E&ESAM, ESAM&ITGA6, and ESAM&PECAM1. Further analysis of the peripheral blood data was conducted using FlowSOM for clustering and subgroup identification, with results visualized through tSNE and UMAP plots (Figure 2E), showing the distribution of disease subgroups across all samples. Additionally, protein expression levels within exosomal subpopulations were quantified and visualized using a heatmap, highlighting the expression patterns and molecular features of each extracellular vesicle subgroup (Figure 2F).

Identification of Asthma-Associated EV Protein Clusters

The protein and molecular densities of each extracellular vesicle (EV) were first analyzed to assess overall distribution patterns (Figure 3A). Detailed comparisons of EV protein expression were then conducted among the three groups: NSA vs Control (Figure 3B), SA vs NSA (Figure 3C), and SA vs Control (Figure 3D). Among these, the SA and NSA comparison was of particular interest, revealing that patients in the SA group showed significantly higher expression of ANXA1 and lower expression of ADAM10 compared to the Control group. However, individual EV proteins alone exhibited limited predictive value for severe asthma, as reflected by low AUC values. To address this, the proteins were clustered based on their expression trends, resulting in 11 clusters, which were further grouped into six main clusters according to their expression patterns (Figure 3E). Clusters with expression trends consistent with disease severity were prioritized for further analysis, with cluster 2, cluster 4, and cluster 6 identified as optimal biomarker sets, and their expression profiles presented in Figure 4A. Recognizing that protein expression alone may not fully capture clinical relevance, lung function data were integrated to exclude proteins with strong expression differences but weak clinical associations. After this refinement, proteins with both biological and clinical predictive value were selected, and their ROC curves were plotted (Figure 4B). For instance, although ANXA1 was highly expressed in the SA group, its predictive performance dropped when combined with clinical data, leading to its exclusion from the final model. Ultimately, ANXA1, TENM2, ITGA4B7, NFASC, ITGAM, LAMP2, and PCDHA1 were selected as predictive markers for distinguishing SA from the control group; ITGA4B7, TENM2, NGFR, and CD20 for NSA vs Control; and PCDHA1, NFASC, NGFR, and IL6 for SA vs NSA.

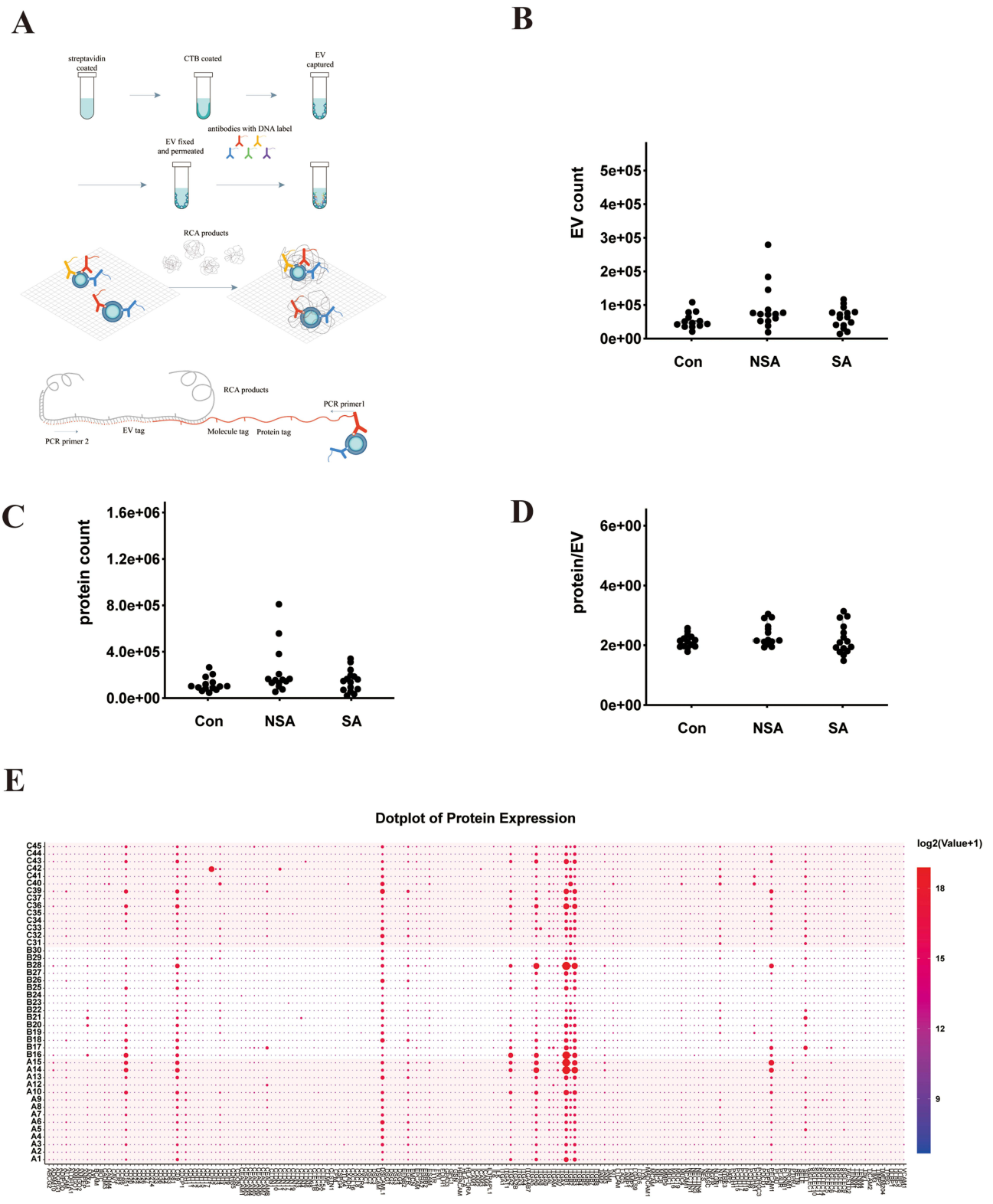

Figure 1 PBA methods of sample processing and basic characterization of exosomes in each group. (**A**) PBA method of processing peripheral blood exosomes from healthy individuals and patients. (**B**) The number of EVs detected in the peripheral blood of each group of subjects in the Con, NSA, and SA groups. (**C**) The total number of proteins detected in the peripheral blood of each group of subjects in the Con, NSA, and SA groups. (**D**) Comparison of the average number of proteins carried per EV detected in the peripheral blood of subjects in the Con, NSA, and SA groups. (**E**) Individual sample protein expression data for each group, and overall protein expression is shown as a dotplot. (n=45).

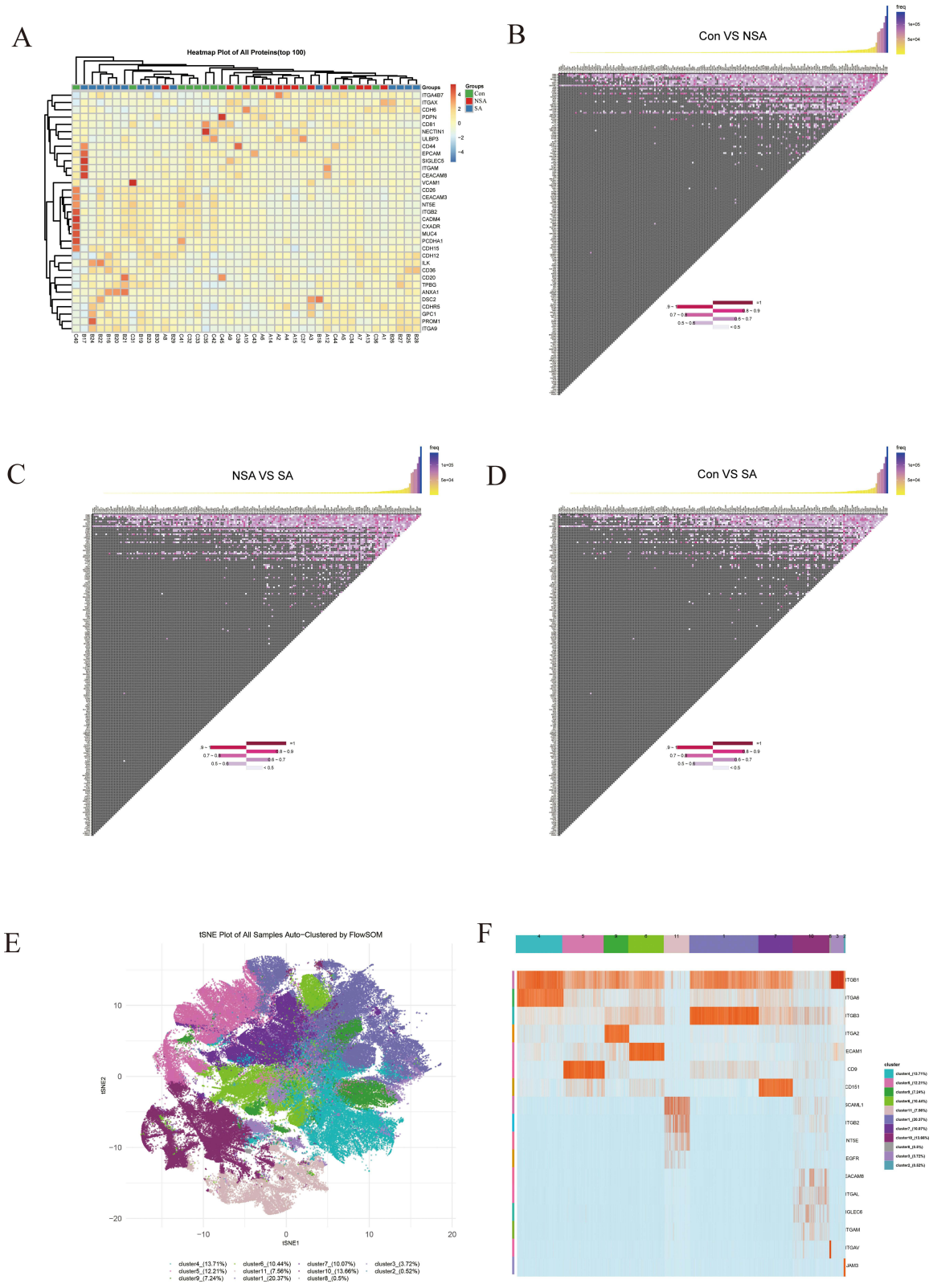

Figure 2 Con, NSA, and SA intergroup expression of differentially expressed proteins, assessment of predictive performance of protein combinations, and visualization and analysis. (**A**) The proteins with expression differences between the sample Con, NSA, and SA groups are shown as heatmaps, and hierarchical clustering between the samples was performed on this basis. (**B**–**D**) The AUC values of proteins detected as biomarkers between Con and NSA groups are reacted in the B. The AUC values are expressed in different colors, and the larger the AUC value is the better the classification performance of the model. The C reacts to the NSA and SA groups, and the D reacts to the SA and Con groups. (**E**) After identifying the downscaling and subgroups of the PBA data using FlowSOM, we visualized the clustering results using tSNE. The specific distribution of each sample and the different disease subgroup samples across all subgroups is shown. (**F**) The expression of exosome subpopulations of proteins was counted, and protein expression abundance was visualized in a heat map to determine the characteristics of each EV subpopulation.

https://doi.org/10.2147/JIR.S556255

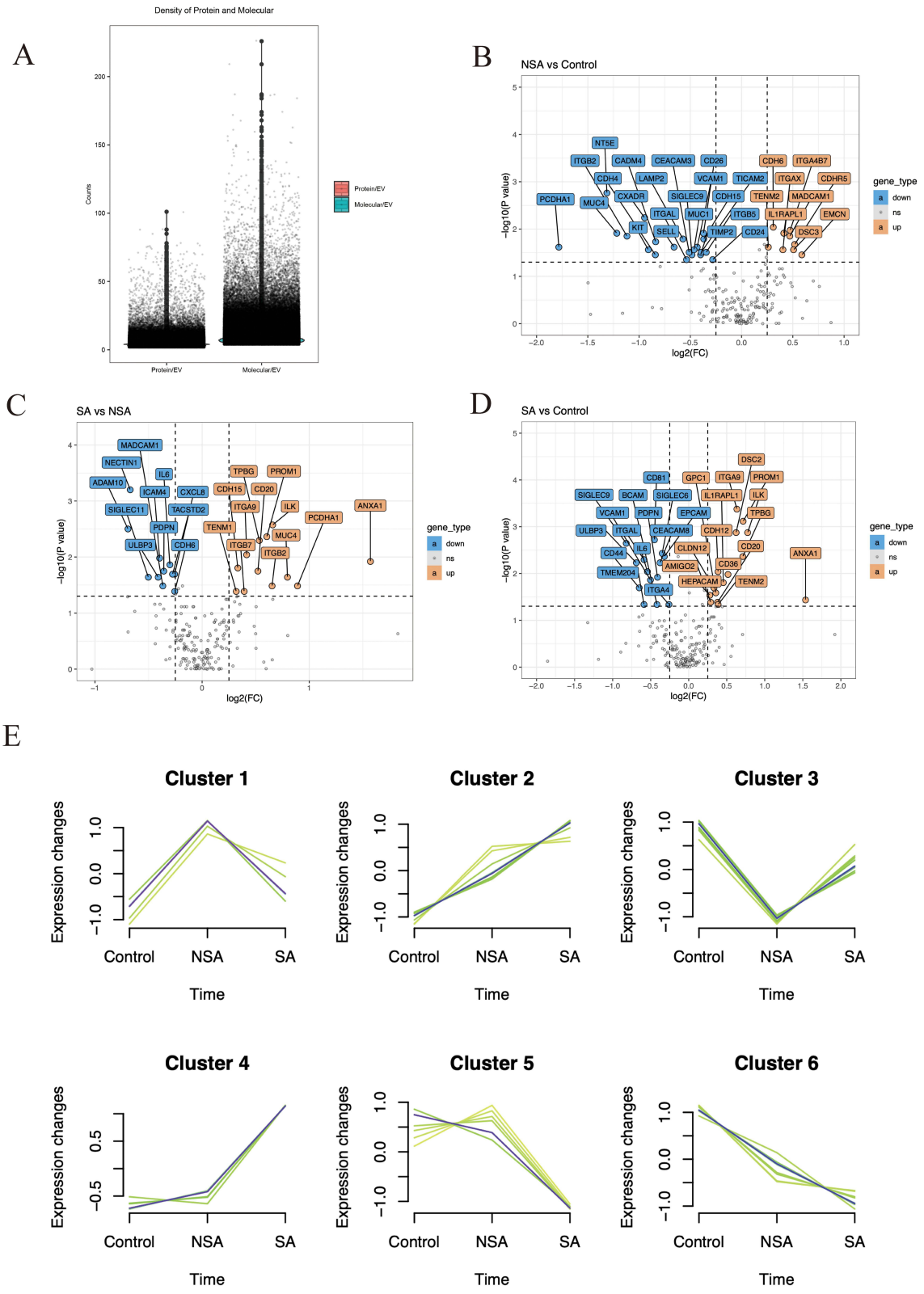

Figure 3 Specific protein expression differences between the Con, NSA, and SA groups and preliminary construction of predictive models. (**A**) protein expression per EV and molecular expression per EV. (**B**–**D**) The B graph reflects proteins with significant expression differences in the Con and NSA groups and contains proteins that are significantly elevated and lowered in the NSA group compared to the SA group.The C graph reflects the SA and NSA groups, and the D graph reflects the differential proteins between the SA and Con groups. (**E**) In order to model severe asthma, it was desired to screen for proteins with the same protein expression trend as the disease trend, so the 11 clusters were divided into 6 clusters.

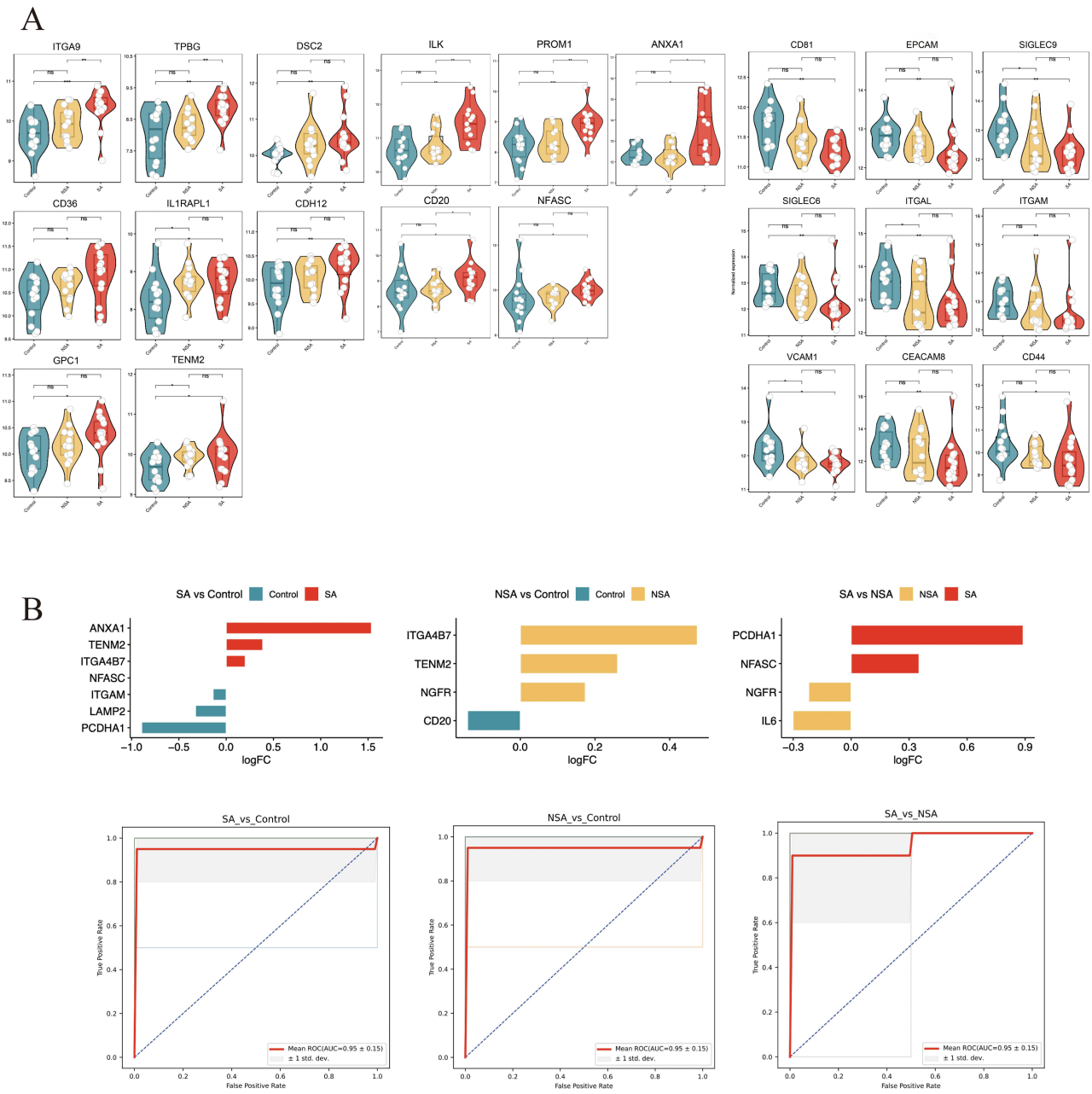

Figure 4 Preliminary predictive modeling of severe asthma using proteins detected in subjects' exosomes. (**A**) The only clusters with consistent expression trends with disease severity were clusters 2, 4, and 6, and proteins with significant expression differences and predictive efficacy for these clusters were selected for specific demonstration. (**B**) The Con group, NSA group, and SA group screened the appropriate proteins, so that the AUC difference in screening efficacy between the groups reached 0.95, and the AUC curves of the screened proteins and the AUC curves of the groups are shown. Statistical significance: ns (P > 0.05), *P < 0.05, **P < 0.01, ***P < 0.001.

Multivariate Integration of Clinical and EV Proteins for Severe Asthma Prediction

Statistical analysis revealed nine parameters demonstrating significant intergroup differences (Figure 5A), including pulmonary function indices (FEV1, FEV1% pred, FEV1/FVC ratio, FEV1/FVC% predicted, DLCO, and DLCO% pred) and clinical biomarkers (ACQ score, blood neutrophil count, and neutrophil percentage). Variables exhibiting superior discriminative capacity (ROC-AUC >0.8) were subsequently incorporated into the predictive algorithm (Figure 5B). Through multivariate regression analysis, we identified three clinical parameters and four extracellular vesicle (EV) proteins that collectively formed the optimal predictive model: FEV1/FVC ratio, blood neutrophil count, DLCO% predicted, IL6, NGFR, NFASC, and PCDHA1. This composite model demonstrated exceptional predictive performance (AUC = 0.97 ± 0.075), as illustrated in Figure 5C.

https://doi.org/10.2147/JIR.S556255

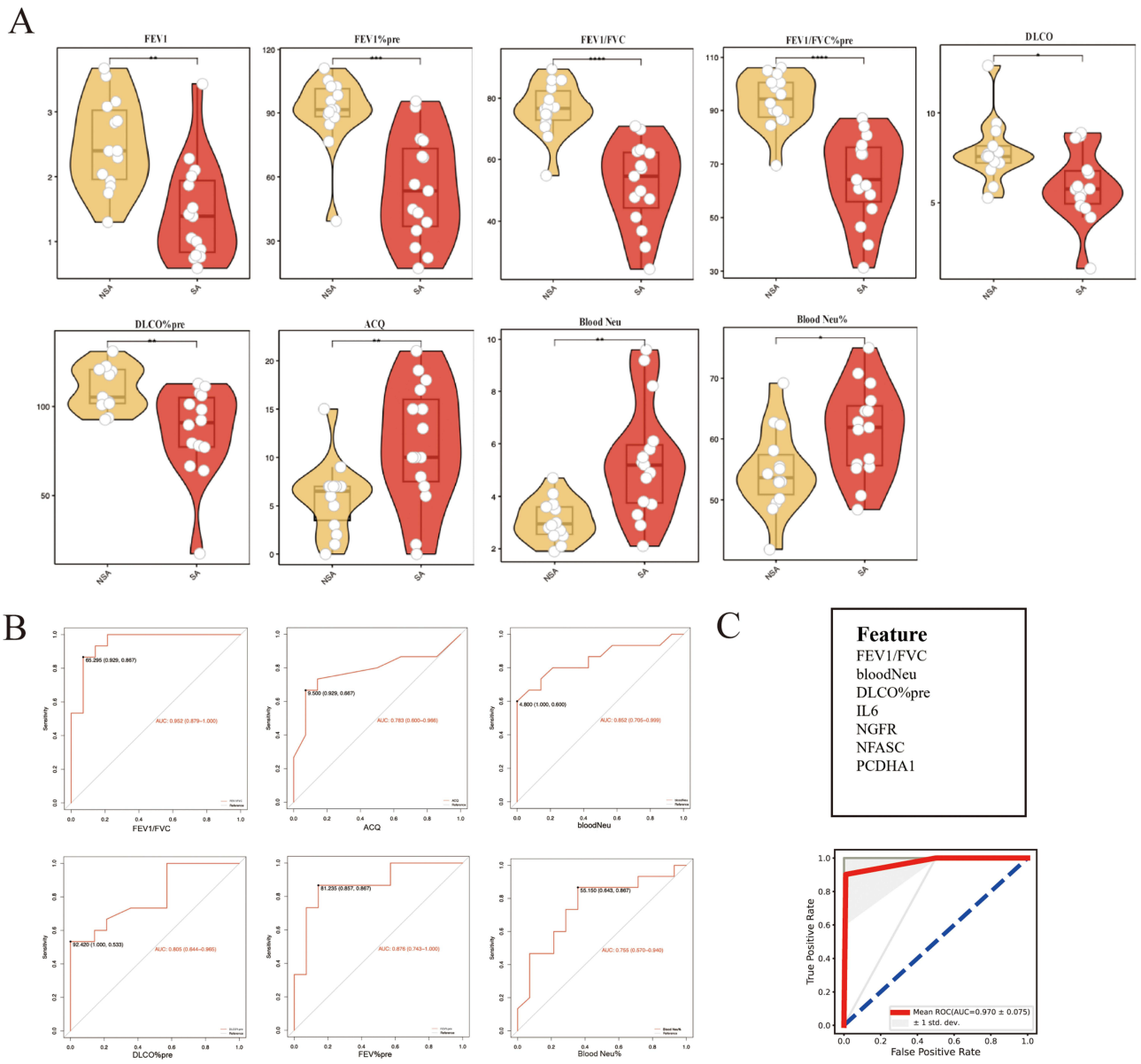

Figure 5 Finalization of a predictive model for severe asthma. (**A**) In order to better screen patients with severe asthma, the focus focused on the differences between the NSA and SA groups, and the clinical data with statistically significant differences between the NSA groups were specifically presented. (**B**) Specifically demonstrating the predictive efficacy of individual clinical variables, only variables with ROC > 0.8 were included in the subsequent prediction portfolio. (**C**) The relevant molecular and clinical data for the final construction of a predictive model for severe asthma were selected and their overall predictive efficacy was calculated. Statistical significance: *P < 0.05, **P < 0.01, ***P < 0.001.****P<0.0001.

Validation in Cellular and Severe Asthma Models

Next, we measured the protein expression in the predicted models associated with cells after Af and LPS interventions. We found that after Af and LPS interventions, the cells exhibited increased NGFR and NFASC expression, as shown in Figure 6A. Subsequent analysis demonstrated concurrent increases in IL-6 secretion after Af and LPS interventions (Figure 6B). The detailed procedures for animal modeling are shown in Figure in Figure 6C. Subsequently, we established a murine model of severe asthma through combinatorial exposure to Af and LPS. H&E and PAS staining in the murine models confirmed marked eosinophilic infiltration and mucus hypersecretion with goblet cell hyperplasia (Figure 6D). Western blot analysis of lung tissue also exhibited significant upregulation of NGFR and NFASC in the severe asthma group (Figure 6E). Comparative assessment of protein expression across both cellular and animal models indicated statistically significant increases in NGFR, NFASC, and IL-6.

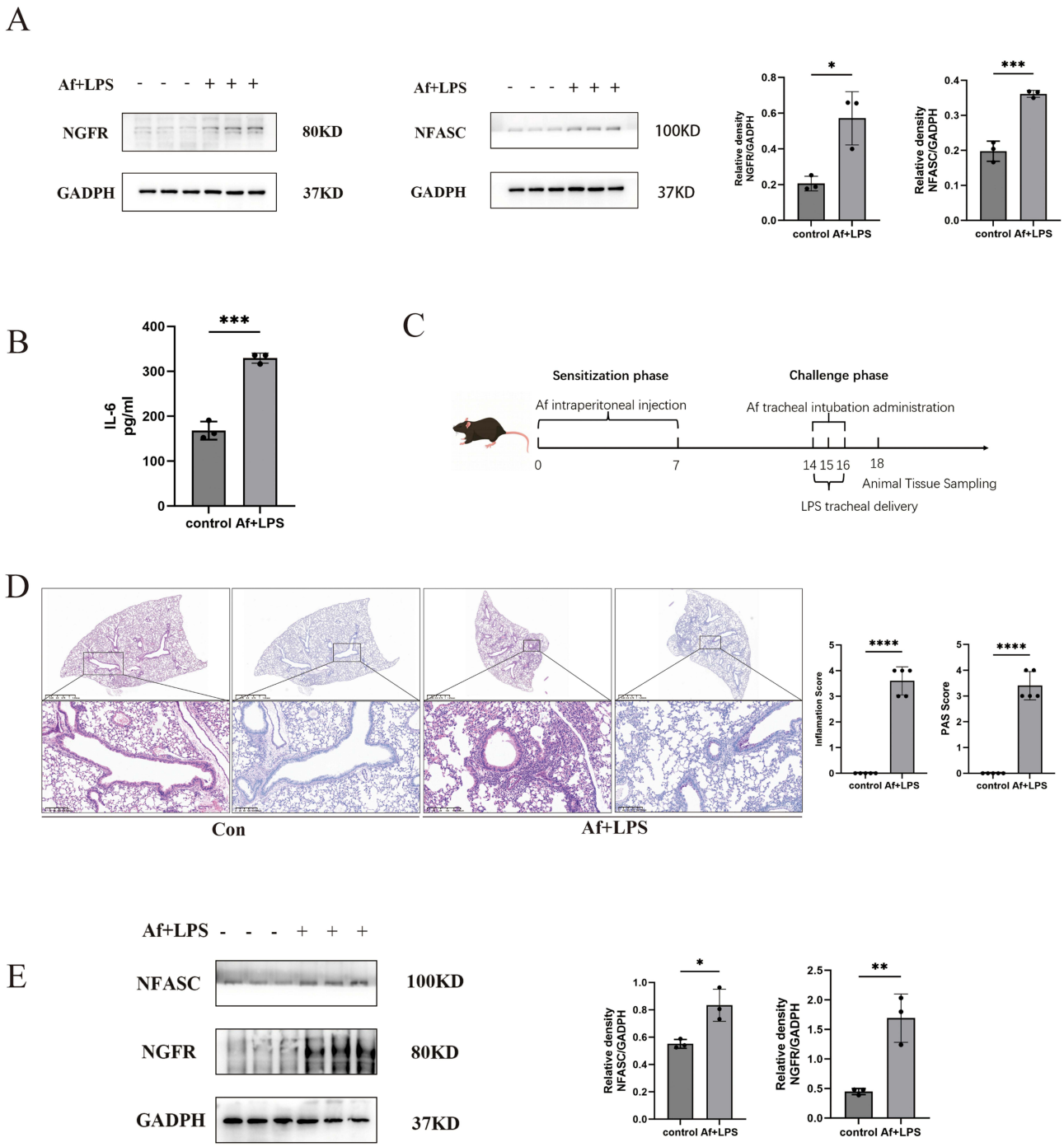

Figure 6 Validation of molecules in predictive models of severe asthma in relevant cellular and animal models constructed by *Aspergillus fumigatus*. (**A**) MLE12 cells were co-intervened with Af (10ug/mL) and LPS (10ug/mL) for 48h and then their protein expression of NGFR,NFASC was measured using Western blot.(n=3) (**B**) MLE12 cells were co-intervened with Af (10ug/mL) and LPS (10ug/mL) for 48h and then their IL-6 protein expression was measured using ELISA. (n=3) (**C**) Detailed modeling methods for C57BL/6 mice. (**D**) Representative H&E and PAS staining images and corresponding inflammation scores as well as PAS scores. Scale bar: 200 μm.(n=5) (**E**) Animal lung tissues between the severe asthma model and the Con group were examined for their protein expression of NGFR and NFASC using Western blot.(n=3) Statistical significance: *P < 0.05, **P < 0.01, ***P < 0.001.****P<0.0001.

Discussion

In this study, by integrating EV proteomics and multi-dimensional clinical parameters, a prediction model for SA (AUC= 0.97± 0.075) was successfully constructed, providing a new paradigm for the precise asthma stratification. Rather than relying on soluble biomarkers in plasma, EV-derived proteomic profiles offer more stable, cell-specific, and functionally

https://doi.org/10.2147/JIR.S556255

relevant information, providing enhanced sensitivity and predictive power for disease classification and individualized treatment strategies.[23] Compared with the traditional single-omics methods, this multimodal strategy fully captures the molecular pathological characteristics of SA (such as IL-6, NGFR) and functional impairment markers (FEV1/FVC), effectively solving the problem of disease heterogeneity. Although EV analysis based on PBA technology identified 9 protein combinations with an AUC greater than 0.8 (such as ITGB3 & CLDN1), its independent predictive efficacy is still limited by the overlap of expression ranges. By integrating lung function parameters (FEV1/FVC, DLCO%pred) and exosome proteins (IL6, NGFR, NFASC, PCDHA1) through machine learning, the specificity of the model was significantly improved, confirming the necessity of the application of the multi-dimensional biomarker framework in complex respiratory diseases.

NGFR, PCDHA1, and NFASC—molecules canonically associated with neuronal patterning—demonstrated consistent upregulation in both SA patients and experimental models. This conserved elevation suggests convergent neuro-immunological mechanisms driving airway pathology. Specifically, the upregulation of NGFR in animal models is consistent with the previously reported nerve growth factor (NGF) -driven airway hyperresponsiveness,[24] while EV-mediated NGFR delivery may amplify the regulatory effect of peripheral nerves on the inflammatory microenvironment. Neurofascin (NFASC), a member of the immunoglobulin superfamily of adhesion molecules, has been implicated in lung cancer metastasis.[25] It emerged here as a novel participant in asthma. The increased expression of NFASC may promote the thickening of the basement membrane by enhancing the communication between smooth muscle-epithelial cells, but the specific mechanism remains to be further explored. Protocadherin-1 (PCDH1), which is important for cell-cell adhesion, is also a susceptibility gene for bronchial hyperresponsiveness.[26–28] In asthma, its abnormal expression may affect the integrity of the airway epithelial barrier, promote allergen penetration, and chronic inflammation. Furthermore, the synchronous increase of IL-6 suggests that EV may act as an "amplifier" of cytokine storms, converting local inflammation into a systemic response through the paracrine pathway, which provides a new molecular perspective for explaining acute exacerbation of SA. While some molecules have been individually documented in respiratory pathogenesis, our study pioneers a systems medicine approach by orchestrating their synergistic interactions with clinical indices, thereby establishing a multi-dimensional predictive framework that bridges molecular insights with actionable clinical stratification for severe asthma.

PBA technology in this study has significant methodological significance. Compared with traditional proteomics, the molecular barcoding technology of PBA can detect low-abundance exosomes with high sensitivity.[29] Notably, the PBA technology effectively avoids the limitation in conventional detection that neurogenic exosomes are "diluted" by inflammatory cell EVs, laying a foundation for subsequent mechanism exploration.[30,31] However, this study also has several limitations. Firstly, the single-center cohort may be insufficiently representative of rare subtypes within SA. Secondly, the cellular sources of NGFR/NFASC still requires single EV sequencing analysis. Finally, the lack of longitudinal data limits the evaluation of the model's ability to predict the progress of SA. Future work should focus on multi-center validation and functional studies in neuro-immune communication, and model-guided clinical trials for selecting biologics biologics.

In conclusion, this study constructed a prediction model for SA integrating the EV proteome (NGFR/NFASC/IL-6) and lung function parameters (FEV1/FVC, DLCO%), breaking through the sensitivity limitations of traditional biomarkers (such as IgE or eosinophils). This discovery provides a new paradigm for the development of SA stratification tools based on liquid biopsy.

Funding

This work was supported by the National Natural Science Foundation of China (82270026 to CZH), "Noncommunicable Chronic Diseases-National Science and Technology Major Project (NO: 2023ZD0506305).

Disclosure

The authors report no conflicts of interest in this work.

References

1. Aboutaleb N, Jamali H, Abolhasani M, Pazoki Toroudi H. Lavender oil (Lavandula angustifolia) attenuates renal ischemia/reperfusion injury in rats through suppression of inflammation, oxidative stress and apoptosis. *Biomed Pharmacother*. 2019;110:9–19. doi:10.1016/j.biopha.2018.11.045
2. Qahtani SYA. Efficacy and safety of intravenous leukotriene receptor antagonists in acute asthma. *Am J Med Sci*. 2023;366(1):22–26. doi:10.1016/j.amjms.2023.04.012
3. Mao Z, Zhu X, Zheng P, et al. Global, regional, and national burden of asthma from 1990 to 2021: a systematic analysis of the global burden of disease study 2021. *Chin Med J Pulmonary Critical Care Med*. 2025;3(1):50–59. doi:10.1016/j.pccm.2025.02.005
4. Huang K, Yang T, Xu J, et al. Prevalence, risk factors, and management of asthma in China: a national cross-sectional study. *Lancet*. 2019;394 (10196):407–418. doi:10.1016/s0140-6736(19)31147-x
5. Global Initiative for Asthma. Global strategy for asthma management and prevention (2024 update). 2024. Available from: https://ginasthma.org/. Accessed December 17, 2025.
6. Zheng Y, Lan L, Lu G, Gao Y-D. Patterns and trends in asthma incidence rates in main Asian and Western countries and their prediction to 2030. *Chin Med J Pulmonary Critical Care Med*. 2024;2(3):188–196. doi:10.1016/j.pccm.2024.08.004
7. Bi J, Min Z, Yuan H, et al. PI3K inhibitor treatment ameliorates the glucocorticoid insensitivity of PBMCs in severe asthma. *Clin Transl Med*. 2020;9(1):22. doi:10.1186/s40169-020-0262-5
8. Zhu T, Li S, Wang J, et al. Induced sputum metabolomic profiles and oxidative stress are associated with chronic obstructive pulmonary disease (COPD) severity: potential use for predictive, preventive, and personalized medicine. *EPMA Journal*. 2020;11(4):645–659. doi:10.1007/s13167-020-00227-w
9. Yin G, Wu X, Wu Y, et al. Evaluating carbon content in airway macrophages as a biomarker of personal exposure to fine particulate matter and its acute respiratory effects. *Chemosphere*. 2021;283:131179. doi:10.1016/j.chemosphere.2021.131179
10. De Filippo M, Castagnoli R, Brambilla I, Leone M, Marseglia GL, Licari A. Management of severe asthma in children: current insights and future directions. *Expert Rev Clin Immunol*. 2025;21(5):587–601. doi:10.1080/1744666x.2025.2493698
11. Huang YJ. The microbiome in asthma heterogeneity: the role of multi-omic investigations. *Immunol Rev*. 2025;330(1):e70015. doi:10.1111/imr.70015
12. Dhar R, Mukherjee S, Mukerjee N, et al. Interrelation between extracellular vesicles miRNAs with chronic lung diseases. *J Cell Physiol*. 2022;237 (11):4021–4036. doi:10.1002/jcp.30867
13. Chen YF, Luh F, Ho YS, Yen Y. Exosomes: a review of biologic function, diagnostic and targeted therapy applications, and clinical trials. *J Biomed Sci*. 2024;31(1):67. doi:10.1186/s12929-024-01055-0
14. Cheema NA, Castagna A, Ambrosani F, et al. Extracellular vesicles in asthma: intercellular cross-talk in TH2 inflammation. *Cells*. 2025;14(7):542. doi:10.3390/cells14070542
15. Ren Y, Zhou M, Li Y, et al. Exosomes derived from M2 macrophages regulate airway inflammation by modulating epithelial cell proliferation and apoptosis. *J Inflamm*. 2025;22(1):19. doi:10.1186/s12950-025-00444-y
16. Cañas JA, Sastre B, Mazzeo C, et al. Exosomes from eosinophils autoregulate and promote eosinophil functions. *J Leukoc Biol*. 2017;101 (5):1191–1199. doi:10.1189/jlb.3AB0516-233RR
17. Pastor L, Vera E, Marin JM, Sanz-Rubio D. Extracellular vesicles from airway secretions: new insights in lung diseases. *Int J Mol Sci*. 2021;22 (2):583. doi:10.3390/ijms22020583
18. Vázquez-Mera S, Miguéns-Suárez P, Martelo-Vidal L, et al. Signature proteins in small extracellular vesicles of granulocytes and CD4(+) T-Cell subpopulations identified by comparative proteomic analysis. *Int J Mol Sci*. 2024;25(19):10848. doi:10.3390/ijms251910848
19. Jia Y, Fang X, Zhu X, et al. IL-13 + type 2 innate lymphoid cells correlate with asthma control status and treatment response. *Am J Respir Cell Mol Biol*. 2016;55(5):675–683. doi:10.1165/rcmb.2016-0099OC
20. Liu X, Li S, Jin J, et al. Preventative tracheal administration of interleukin-27 attenuates allergic asthma by improving the lung Th1 microenvironment. *J Cell Physiol*. 2019;234(5):6642–6653. doi:10.1002/jcp.27422
21. Yue M, Tao S, Gaietto K, Chen W. Omics approaches in asthma research: challenges and opportunities. *Chin Med J Pulm Crit Care Med*. 2024;2:1–9. doi:10.1016/j.pccm.2024.02.002
22. Niu C, Xu Y, Schuler CL, et al. Evaluation of risk scores to predict pediatric severe asthma exacerbations. *J Allergy Clin Immunol Pract*. 2021;9 (12):4393–4401.e4398. doi:10.1016/j.jaip.2021.08.030
23. Woith E, Fuhrmann G, Melzig MF. Extracellular vesicles—connecting kingdoms. *Int J Mol Sci*. 2019;20(22). doi:10.3390/ijms20225695
24. Ogawa H, Azuma M, Umeno A, et al. Singlet oxygen -derived nerve growth factor exacerbates airway hyperresponsiveness in a mouse model of asthma with mixed inflammation. *Allergol Int*. 2022;71(3):395–404. doi:10.1016/j.alit.2022.02.005
25. Samulin Erdem J, Arnoldussen YJ, Skaug V, Haugen A, Zienolddiny S. Copy number variation, increased gene expression, and molecular mechanisms of neurofascin in lung cancer. *Mol Carcinog*. 2017;56(9):2076–2085. doi:10.1002/mc.22664
26. Faura Tellez G, Vandepoele K, Brouwer U, et al. Protocadherin-1 binds to SMAD3 and suppresses TGF-β1-induced gene transcription. *Am J Physiol Lung Cell Mol Physiol*. 2015;309(7):L725–735. doi:10.1152/ajplung.00346.2014
27. Koning H, Postma DS, Brunekreef B, et al. Protocadherin-1 polymorphisms are associated with eczema in two Dutch birth cohorts. *Pediatr Allergy Immunol*. 2012;23(3):270–277. doi:10.1111/j.1399-3038.2011.01201.x
28. Koppelman GH, Meyers DA, Howard TD, et al. Identification of PCDH1 as a novel susceptibility gene for bronchial hyperresponsiveness. *Am J Respir Crit Care Med*. 2009;180(10):929–935. doi:10.1164/rccm.200810-1621OC
29. Wang C, Lu Z, She G, et al. The identification of FN1 as an early diagnostic marker for recurrent abortion by single-exosome profiling. *Int J Gen Med*. 2025;18:691–702. doi:10.2147/ijgm.S487632
30. Wang Y-W, Tan P-C, Li Q-F, Xu X-W, Zhou S-B. Adipose tissue protects against skin photodamage through CD151- and AdipoQ- EVs. *Cell Commun Signal*. 2024;22(1):594. doi:10.1186/s12964-024-01978-z
31. Zhang S, Liao A, Wang Y, et al. Profiling expressing features of surface proteins on single-exosome in first-episode Schizophrenia patients: a preliminary study. *Schizophrenia*. 2024;10(1):84. doi:10.1038/s41537-024-00510-z